GEOLOCATION OF DEVICES IN LOW-POWER WIDE-AREA LORA NETWORK

Ladislav Zemko*, Daniel Hroš, Alexander Valach, Marek Galinski, Pavel Čičák

Institute of Computer Engineering and Applied Informatics, Faculty of Informatics and Information Technologies, Slovak University of Technology, Bratislava, Slovakia

*E-mail of corresponding author: ladislav.zemko@stuba.sk

Ladislav Zemko 0000-0002-5635-265X,
Alexander Valach 0000-0001-8299-0914,
Pavel Čičák 0000-0002-3021-1971
Daniel Hroš 0009-0002-7850-7509,
Marek Galinski 0000-0001-6622-526X,

Resume

This article is focused on the geolocation possibilities in low-power deployments. A novel Logarithmic Distance Path Loss Model with a Memory (LDPL-M) algorithm is proposed to enhance the accuracy of determining the location of end devices. The proposed solution, utilizing the RSSI-based trilateration, proved more accurate by 24.54% compared to the conventional Logarithmic Distance Path Loss Model (LDPL). Compared to the Global Positioning System (GPS), the power consumption was 48.8% lower. These findings make it suitable for energy-harvesting deployments, environments with limited power supply, or generally hard-to-reach areas, covering various logistics, transportation, or asset tracking scenarios. Overall, in this article, a valuable insight into the geolocation, focusing on the accuracy and efficiency, is provided.

Article info

Received 19 May 2025
Accepted 6 August 2025
Online 19 September 2025

Keywords:

LoRa
LoRaWAN
geolocation
IoT
LPWAN
RSSI
trilateration

Available online: https://doi.org/10.26552/com.C.2025.050

ISSN 1335-4205 (print version)
ISSN 2585-7878 (online version)

1 Introduction

LoRa technology belongs to the field of Low-Power Wide-Area Networks (LPWANs). It enables the connection of end devices that send small data volumes over long distances several times a day with minimal energy consumption. They last 5 to 10 years on a single charge and can be placed even in hard-to-reach places without access to electricity.

New opportunities for the geolocation of end devices are presented by the Internet of Things (IoT) environment. Position can be traditionally determined by the Global Navigation Satellite Systems (GNSS), including the Global Positioning System (GPS), via a constellation of multiple satellites orbiting the Earth. Navigation messages are continuously transmitted by the satellites to the end devices, allowing their position to be calculated. The GPS-independent systems are currently being considered a promising research area. An uninterrupted connection between the receiver and the satellite is required by GNSS, which affects the power consumption. The signals sent can be blocked by obstacles and weather changes, resulting in a certain error. Therefore, such systems are not suitable for the indoor use [1].

The LPWANs' properties have the potential to enable the device geolocation, while maintaining low power consumption [2-5]. LoRa is a wireless technology promoted by the LoRa Alliance. It is based on a proprietary Chirp Spread Spectrum (CSS) modulation, which means a regular change in signal frequency, increasing or decreasing over time, operating on the physical layer of the Open Systems Interconnection (OSI) model [3, 6]. It uses the freely available Industrial Scientific and Medical (ISM) band for data transmission, so observing the so-called duty cycle (DC) is necessary. The DC limits the time a device can transmit. In our use case, this is 1% of time, which equals 36 seconds per hour [7-8].

Above the LoRa physical modulation operates the LoRaWAN protocol, ensuring bi-directional communication. LoRaWAN is standardized by the LoRa Alliance and has the possibility of roaming, but with the costs of higher energy consumption, compared to

other protocols, e.g., LoRa@FIIT [7, 9-11]. A typical implementation of a LoRaWAN network consists of end devices (simple battery-powered sensors), gateways, a network server, and an application server. In most applications, end devices are autonomous, connected in a star[1] topology, sending the collected data via LoRa technology to all the gateways within their range. After the gateway receives a message, it immediately adds metadata to it: timestamp, Received Signal Strength Indicator (RSSI), Signal to Noise Ratio (SNR), and others, which are crucial for the geolocation in wireless networks [9].

Unlike the GNSS, geolocation use cases in LoRaWAN network are specific to the standardized roaming architecture, allowing end devices to use the gateways of different networks and therefore to send messages between different LoRaWAN operators. As the uplink communication is not bound to a specific gateway, it improves the coverage and capacity, which has the potential to reduce the costs and energy consumption [6, 12]. The main problem with the GPS-equipped devices is the power consumption of around 30-50 mA. A typical power consumption of a LoRaWAN device is about 2.8 mA in the active state, 38.9 mA during uplink transmission, and 14.2 mA during downlink reception [13].

The research was focused on the LoRaWAN protocol and the LoRa technology, which belong to the category of LPWANs. The findings are not limited to this specific technology but are generally applicable to wireless communication technologies. The geolocation accuracy in LoRa networks depends on types of devices and communication parameters, as well as the method used, i.e., triangulation, trilateration, and multilateration. A novel Logarithmic Distance Path Loss Model with Memory (LDPL-M) algorithm is proposed, considering not only the actual end device's location, but the previous locations, as well. The geolocation is determined by the RSSI-based trilateration. Compared to the standard methods using GNSS, LPWANs allow the location of end devices to be determined over a wide area with minimal power consumption. Results have shown that this modification improves the overall geolocation accuracy for both the stationary and mobile devices. The benefit of this solution is that no additional communication overhead is required.

The main contribution of this article lies in the following:

- Research in the field of LPWANs and suitable geolocation methods: LPWANs with the focus on the LoRa technology are described, and an overview of the methods applicable in LoRa network with low power consumption in mind is provided throughout the research.
- Proposal of the LDPL-M algorithm: The LDPL-M algorithm for the geolocation of the end devices based on the trilateration using RSSI is proposed. Compared to the existing solutions, it computes the end device's position using not only the current location, but considers n previously determined locations, which improves the overall accuracy. The accuracy, or the error, of the proposed algorithm is also measured and compared to other methods, including the GPS sensor data.

The article is organized as follows: in Section 2, related work and the geolocation techniques applicable in LPWANs are described. In Section 3, a private LoRaWAN network and its components are described, and the methodology of data collection and processing in both the private and public provider networks is explained. A method for estimating the initial position is also described, and the LDPL-M algorithm is proposed to improve geolocation accuracy. The web interface for displaying the end device's position on the map and the software architecture of the solution are also described in this section. The dataset gathered is described in Section 4. In Section 5, the achieved results are discussed, and the accuracy of geolocation is compared. Additionally, the impact of utilizing the GPS sensor on power consumption is assessed. In Section 6, the limitations of the solution and potential future research directions are discussed. Finally, the article is concluded in Section 7.

2 Related work

Geolocation of LoRa end devices is an active research area, with several proposed methods and algorithms to enhance the overall accuracy. Recent studies have demonstrated that machine learning algorithms and hybrid methods combining different techniques offer promising results [6]. Furthermore, the proper deployment and positioning of LoRa gateways can significantly influence geolocation accuracy, so further research is still required to optimize the gateway placement in different environments. Several studies have examined the deployment and type of LoRa gateways and their influence on geolocation accuracy, including a study by Podevijn et al. [14] that examined the impact on geolocation accuracy in an urban environment.

Although the considerable research has been done on geolocation in LoRa networks, there is a need for more publicly available data on this topic in Bratislava, Slovakia. This study aim was to examine the accuracy and feasibility of geolocation in a real-world environment and provide insights into the factors that could impact the precision.

The three most common geolocation techniques used in the wireless networks are multilateration, trilateration, and triangulation, which require knowledge of the location of reference points (gateways). The choice of the appropriate technique depends on the use case and the available information about the end device [13].

[1] star-of-stars

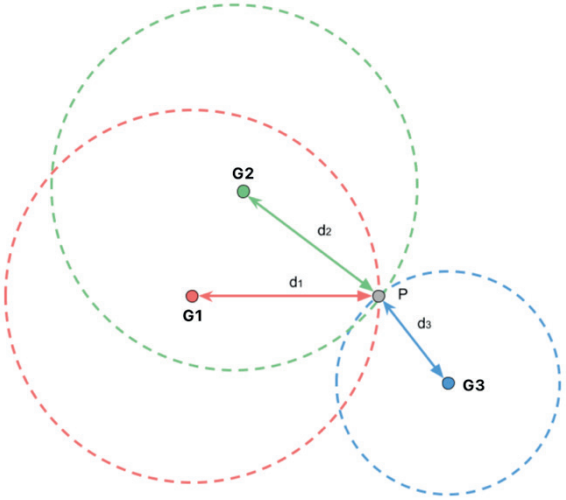

Figure 1 *Position calculation using trilateration [15]*

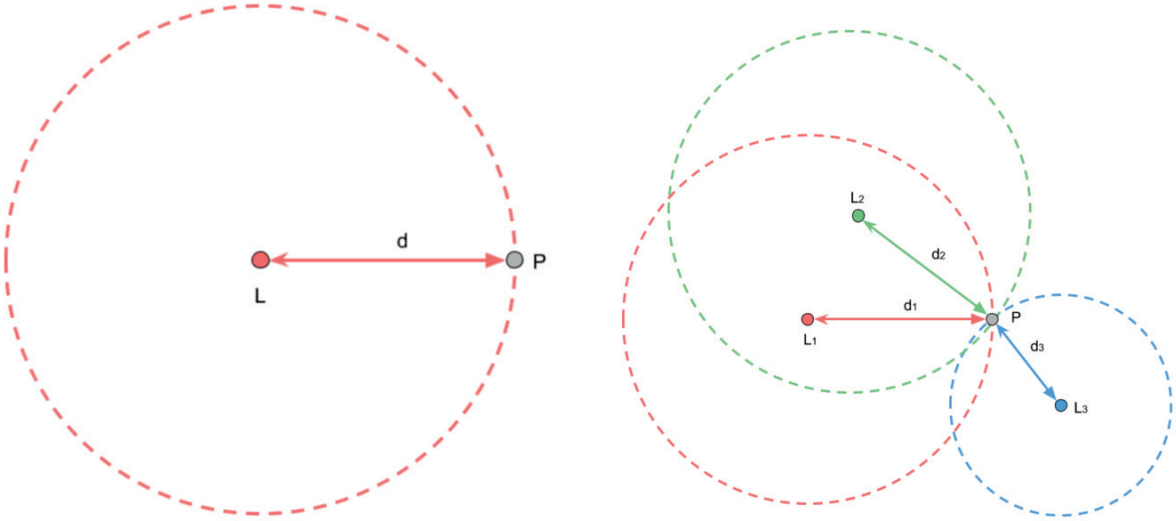

Figure 2 *Representation of distance from (a) single reference point and (b) multiple reference points [15]*

The trilateration uses the distance between the transmitting device and each reference point in its calculation, as shown in Figure 1. The distance between devices can be calculated in two ways:

- Based on the Time of Arrival (ToA),
- Based on the RSSI value.

For the correct calculation of the distance in the ToA method, it is essential to correctly determine the transmission time between devices. The proper determination requires time synchronization between the end device and all the reference points in the network. Time synchronization on end devices requires additional communication and thus can increase power consumption. Trilateration using ToA for determining the end device's location is therefore unsuitable for LPWANs [13, 16].

The multilateration does not require knowledge of the device's distance from each reference point, but only the difference of distances from each reference point to the device. The Time Difference of Arrival (TDoA) between the end device and the reference points is used to calculate the distance difference. Thus, this method requires time synchronization only between the reference points [13]. Even a small error in the time synchronization (1 µs) can cause a significant error in determining the position of the end device (300 m) [1].

The triangulation uses the geometry of a triangle defined by the two angles of the signal Angle of Arrival (AoA) for calculation. However, AoA measurements are not suitable for geolocation in the LoRa network due to the accumulating angle error with increasing distance from the reference points [13].

In LPWANs, the multilateration (TDoA values can be determined) and trilateration (RSSI value available in LoRaWAN packet) can be used to calculate the position of the end device. Studies show better accuracy of TDoA over RSSI [13, 17]. As the gateway clocks are synchronized using the Network Time Protocol (NTP),

only the precision at milliseconds is achieved, which is not sufficient for the TDoA-based geolocation.

The trilateration can be used to estimate location using RSSI. To simplify the calculations, the intersection of circles is in the Cartesian plane. Referring to Figure 2, the device's P location is intended to be determined using a reference point L whose location is known. Based on a single reference point, the location of the device P cannot be determined; it is possible to estimate the distance d between P and L using the RSSI-based techniques, as shown in Figure 2a. Each point is a potential candidate for P at this distance. For the correct determination of P, at least three circles whose intersection is at a single point are required. This point represents the actual location of the device, shown in Figure 2b. Multiple circles using various reference points are created, each at a known location L_i. For each reference point, it is possible to determine the distance d_i from P [15].

The equation for a circle in a plane:

$$(x - c_x)^2 + (y - c_y)^2 = d^2, \tag{1}$$

where the point (x, y) on the Cartesian plane lies on a circle of radius d centered on (c_x, c_y). From Equation (1), it is possible to derive the equations for the circles generated by the reference points. Each reference point has a known location expressed by latitude and longitude coordinates (ϕ_i, λ_i). The intersection of the circles can be obtained by solving the system of three linear equations, thereby determining the location of the point $P = (\phi, \lambda)$ [15, 18]:

$$\begin{aligned} (\phi - \phi_1)^2 + (\lambda - \lambda_1)^2 &= d_1^2, \\ (\phi - \phi_2)^2 + (\lambda - \lambda_2)^2 &= d_2^2, \\ (\phi - \phi_3)^2 + (\lambda - \lambda_3)^2 &= d_3^2. \end{aligned} \tag{2}$$

This method is mathematically correct, however, several problems were encountered that make it impractical. In the real world, a set of equations may not have a solution, as the circles may not intersect at a single point due to measurement error. For example, in [19], the authors tried to create a prototype of a wireless network in a coal mine to navigate miners out of the mine in case of an emergency. The geolocation proved to be unsuccessful due to the significant environmental interference, which caused errors in the measurement of the distance of the end devices from the reference points. In the same way, the measurements from more than three reference points cannot be used in the analytical approach. Therefore, this problem is approached more like an optimization problem by searching for a point $X = (\phi_x, \lambda_x)$ that provides the best approximation to P. Using the Mean Squared Error (MSE) calculation, it can be verified how well the point X replaces the point P [19]:

$$\frac{\sum_{i=1}^{n} [d_i - dist(X, L_i)]^2}{n}, \tag{3}$$

where $dist(X, L_i)$ is a distance between point X and reference point L_i.

If this distance coincides with the corresponding distance d_i, it contributes minimal error to the total error, or none at all (it is assumed that X is indeed P). The use of squares eliminates the mutual subtraction of positive and negative errors. The optimization algorithm should be able to converge to a reasonable result. Providing an estimate of the initial position of X can speed up its execution. The advantage is the possibility to use any number of reference points [15].

3 Proposed solution

A novel LDPL-M algorithm for determining the end devices' location is described in this section, including architecture, data collection and processing, initial position estimation, the LDPL-M algorithm itself, and results achieved for the stationary and mobile devices. The requirements for the proposed technique and its evaluation were the following:

1. The geolocation of end devices powered by a limited power source. The location of end devices is determined by the RSSI-based trilateration in a LoRaWAN network.
2. Comparison of the accuracy of existing geolocation methods within the trilateration. To compare the accuracy of individual geolocation techniques, a graph of the Cumulative Distribution Function (CDF) and a table of error rates of particular methods are used in each percentile. At the same time, using different methods, depending on specific use cases, may require different levels of accuracy.
3. Verification of the LDPL-M accuracy. An external GPS sensor is utilized to provide a reference value for the actual location of the end device, with an accuracy of 15 mm.
4. Visualization of the end devices' location on the map. As a part of the research, a web interface that displays the last recorded location of the end device, along with information about the time of the most recent location update, was created.
5. Contribution to future research and community. The creation of a publicly available dataset contributes to the field of LPWANs and geolocation.

This research is focused exclusively on the geolocation by the RSSI-based trilateration, due to the hardware limitations. The basic principle of determining the end device's location based on the RSSI consists of associating the path loss with the distance between the transmitted and received signal. Path loss represents the loss of signal strength that occurs during the transmission through a communication medium and obstacles, such as air or a wall. Path loss can be calculated using the link budget, which includes all signal gains and losses during transmission from the

transmitter to the receiver. This budget is defined by [20-21]:

$$P_{Rx} = P_{Tx} + G_{Rx} + G_{Tx} - L_{PL}, \quad (4)$$

where: P_{Rx} is a signal strength at the receiver,
P_{Tx} is a signal strength at the transmitter,
G_{Rx} is a gain of the antenna used by the receiver,
G_{Tx} is a gain of the antenna used by the transmitter,
L_{PL} is a path loss.

The path loss is calculated by substituting the RSSI value into P_{Rx} in Equation (4). The path loss can be subsequently associated with the distance the signal has traveled through several models:

Free-space Path Loss Model (FSPL): The main idea is that the strength of a received wireless signal passing through free space decreases quadratically with increasing distance from the sender [22]:

$$P_{Rx}(d) = \frac{P_{Tx} G_{Tx} G_{Rx} \lambda^2}{(4\pi d)^2}, \quad (5)$$

where: $P_{Rx}(d)$ is a signal strength at receiver at a distance d,
λ is a wavelength,
d is a distance between receiver and sender.

A more appropriate notation of the model is in units of decibels (dB):

$$FSPL(d) = 20\log_{10}(d) + 20\log_{10}(f) + \\ + 20\log_{10}\left(\frac{4\pi}{6}\right), \quad (6)$$

where: $FSPL(d)$ is a path loss at a distance d,
d is a distance between receiver and sender,
f is a carrier frequency,
c is a speed of light.

Logarithmic Distance Path Loss Model (LDPL): In reality, most signals are received in an environment without direct visibility of devices (Non-Line of Sight, NLoS), which results in interference, especially in built-up areas. Interference is caused by reflections from buildings, weather, and other variables, considering the utilization of FSPL is more of an idealization. Based on empirical evidence, it is more appropriate to estimate the distance according to the LDPL formula [16, 21]:

$$L_{PL}(d) = L_{PL}(d_0) + 10\beta\log\left(\frac{d}{d_0}\right) + X_\sigma \quad (7)$$

where: $L_{PL}(d)$ is a path loss at a distance d in dB,
$L_{PL}(d_0)$ is a path loss at a reference distance d_0 in dB,
β is a path loss exponent - an empirical constant dependent on the environment,
X_σ is a path loss random variable from the shading factor with zero Gaussian mean value and standard deviation σ in dB.

By substituting L_{PL} from Equation (4) into Equation (7), the distance d can be estimated if the values of the parameters β and $L_{PL}(d_0)$ are available. These values can be obtained by performing empirical measurements - machine learning methods by fitting a logarithmic curve are used to describe the best the data obtained by the measurements. The values of the parameters β and $L_{PL}(d_0)$ depend on the environment [23].

In addition to the mentioned models, there are other models, such as Okumura-Hata, Cost 231, or IMT-2000 [21].

To improve the results of the RSSI-based geolocation, the RSSI can be substituted with the Estimated Signal Power (ESP) with the environmental interference considered. ESP is beneficial due to the characteristics of LoRa networks, in which a relatively noisy signal can be received (in practice, the gateway manages to decode even frames with the RSSI of approximately –120 dBm) [24]. The ESP equation can be written in the logarithmic form [21, 25]:

$$ESP_{(dBm)} = RSSI_{(dBm)} + SNR_{(dB)} - \\ - 10\log_{10}(1 + 10^{0.1\,SNR_{(dB)}}). \quad (8)$$

The ESP can be processed the same way as the RSSI, and therefore substituted into P_{Rx} in Equation (4), and then used to calculate the distance between the end device and the gateway using Equation (7). For most of the previous works, which determined the position of the RSSI device, determining the position in a smaller area or sparsely built-up areas with minimal environmental interference was specific. Any environmental obstacle seriously affects the geolocation accuracy [21]. It can therefore be concluded that such device geolocation is more suitable for a smaller area and environments with direct visibility of devices (Direct Line of Sight, DLoS).

3.1 Architecture

In this section, the primary focus is on the architecture of the private LoRaWAN network. Unfortunately, during the research, it was not possible to access the architecture of the public provider network, so it cannot be discussed in more detail. Figure 3 shows the locations of gateways within the private network. All gateways were strategically placed to form a polygon and maintain DLoS with the end device. The highlighted polygon illustrates the area in which the end device was able to move during the data collection. The network consisted of the following components:

- End device: Development Kit LilyGo TTGO ESP32 with SX1276 LoRa Chip and built-in NEO-6M GPS

module. The device was programmed to periodically transmit uplink (from the end device to the network server) messages at 868 MHz frequency band. The LMIC-node library [26] was used.

- Network server: Messages sent from end devices received by gateways were sent over the Internet to the ChirpStack network server. This open-source implementation provided a web interface to manage gateways, end devices, and applications [27]. Using the ChirpStack network server, all the measured data was downloaded and processed in JavaScript Object Notation (JSON) format.
- Gateways: During the data collection phase, 8 Raspberry Pi microcomputers were utilized as gateways within the network. These microcomputers were attached a compatible backplane connecting the Raspberry Pi to an iC880A LoRaWAN concentrator with an 868 MHz antenna. Each gateway was running the Raspberry Pi OS operating system. One of the key advantages of using Raspberry Pi

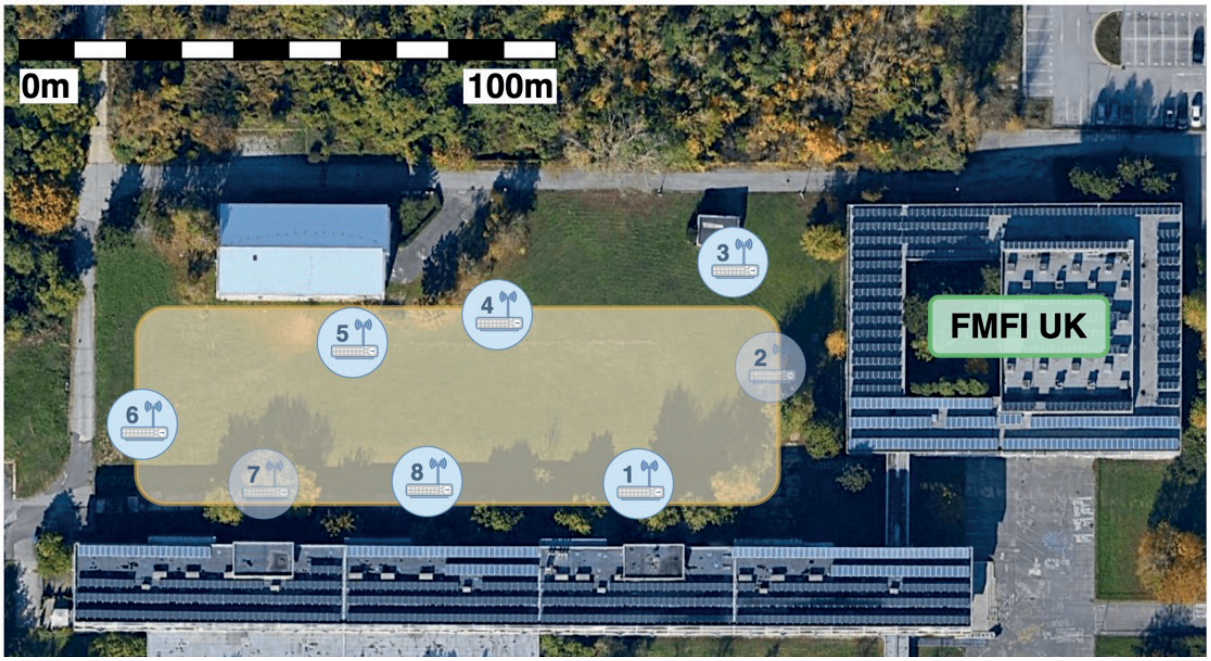

Figure 3 *Gateways position - Google Maps data*

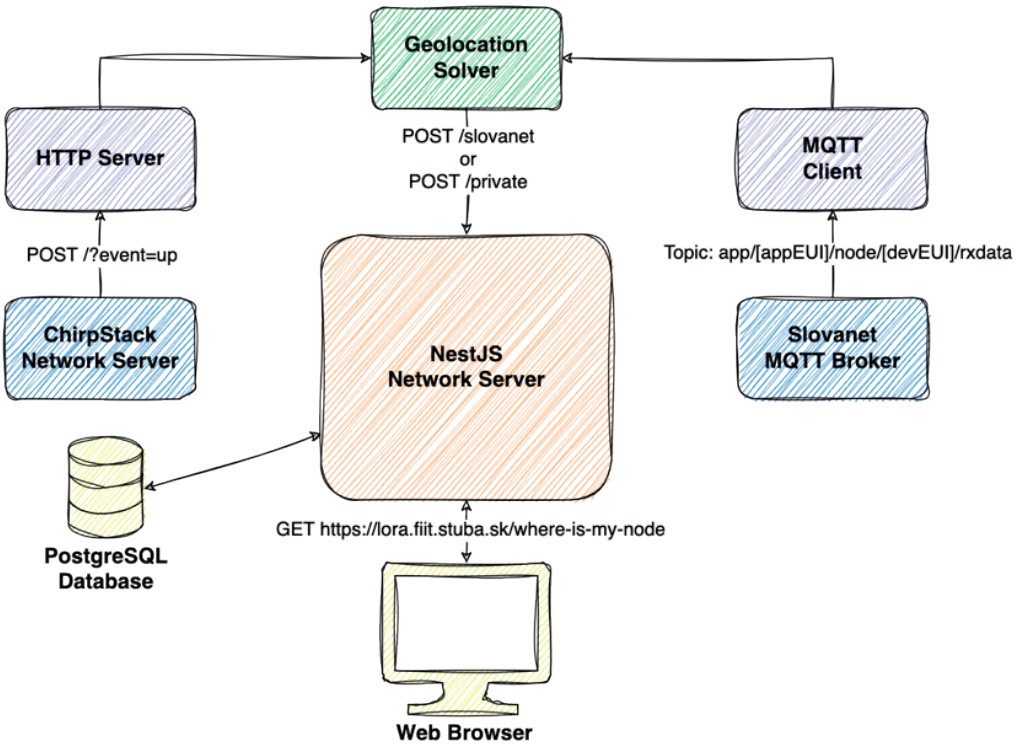

Figure 4 *Software architecture*

gateways was their mobility, as they can be powered by power banks.

During the data collection and experiments, a microservice architecture, shown in Figure 4, was used, which consisted of the following services:

- Hypertext Transfer Protocol (HTTP) Server: A minimalist HTTP server programmed in Python. The ChirpStack network server allows the captured uplink messages from the end device to be sent to any Internet Protocol (IP) address in real time using the HTTP protocol. The task of the HTTP server is to capture messages from the ChirpStack network server and then forward them via the HTTP protocol to a Geolocation Solver service.
- Message Queuing Telemetry Transport (MQTT) Client: A simple MQTT subscriber. The public provider sends the real-time uplink messages from the end device to this topic. When implementing the subscriber, it is suggested to use the *paho.mqtt* Python module. The task of this service is similar to the previous case, i.e., to forward uplink messages to the Geolocation Solver.
- Geolocation Solver: This service estimates the end devices' position in both networks separately. It uses the LDPL-M algorithm further described in the following sections. This service is implemented using a Python *http* module. After calculating the end device's position, the coordinates are sent to the NestJS web server via HTTP.
- NestJS Web server: A simple web server storing information about the end devices' location in the database (for each device in both networks separately). This service also contains the "Where is my node ?" user interface described in Section 4.8 in more detail.

3.2 Initial position estimation

Algorithms that determine the location of end devices typically need an initial estimate of the starting position. The accuracy can be slightly lower, as the algorithms should eventually converge to more accurate results. The Weighted Centroid (WC) of the gateways that received the signal from the end device was used for the initial estimate. The path loss for the given gateway determined the weight. The inspiration for this idea came from a solution proposed by Bissett [21] - weight was linked to the ToA. It was assumed that a lower path loss value indicates a gateway closer to the end device and vice versa. Based on this assumption, the weight for each gateway was calculated as follows:

$$w = \frac{L_{PLn} - L_{PLi}}{L_{PLn}} + \frac{c}{n}, \tag{9}$$

where: w_i is a weight of the ith gateway's influence on the gravity center calculation,
L_{PLi} is a path loss of the ith gateway of the given transmission,
L_{PLn} is the largest path loss of the given transmission,
c is a constant adding minimum weight for each gateway,
n is a number of gateways that received the uplink message.

The resulting formula for calculating the estimated initial value is as follows:

$$\begin{pmatrix} \hat{x} \\ \hat{y} \end{pmatrix} = \sum_{i=1}^{n} \hat{w}_i \begin{pmatrix} x_i \\ y_i \end{pmatrix}, \tag{10}$$

where: $\begin{pmatrix} \hat{x} \\ \hat{y} \end{pmatrix}$ is a weighted centroid of gateways' gravity, i.e., the estimated starting position of the end device.

In addition to estimating the initial position, the weighted centroid was used as one of the techniques to determine the actual position.

3.3 Map projection

Coordinates define the location on the ground. There are two coordinate systems: the Geographic Coordinate System (GCS) and the Projected Coordinate System (PCS). The GCS defines the position in angles based on latitude and longitude from the center of the Earth [28]. The PCS, or Cartesian Coordinate Systems (CCS), represents the three-dimensional GCS in two dimensions by projecting and leveling the Earth's surface onto a plane. During the projection, distortions occur (shape, area, distance, or direction). No kind of projection preserves all four geographic features at the same time. Each projection tries to preserve some geographical feature, but with the knowledge of compromising other features. For this reason, many different projections are divided into three main projection systems: cylindrical, conical, and planar. The main focus is on the cylindrical projection, as with this type of projection, the lines of latitude and longitude remain parallel to the x and y axes [21, 28].

Figure 5a shows the Mercator projection, one of the most popular and used cylindrical projections. It is used in most map applications, such as Google Maps or OpenStreetMap. However, this type of projection distorts areas further from the equator. The Equidistant projection, shown in Figure 5b, maintains constant distances along both lines of latitude and longitude, and thus is more suitable for experimental geolocation using the RSSI-based trilateration. In Equidistant projection, it is possible to directly assign the displayed pixel on the map to the corresponding geographic location on the Earth.

By a simple calculation, the GCS can be converted to the PCS, i.e., the latitude and longitude *(λ, ϕ)* can be converted to coordinates *(x, y)* in the Cartesian plane [21, 28-29]:

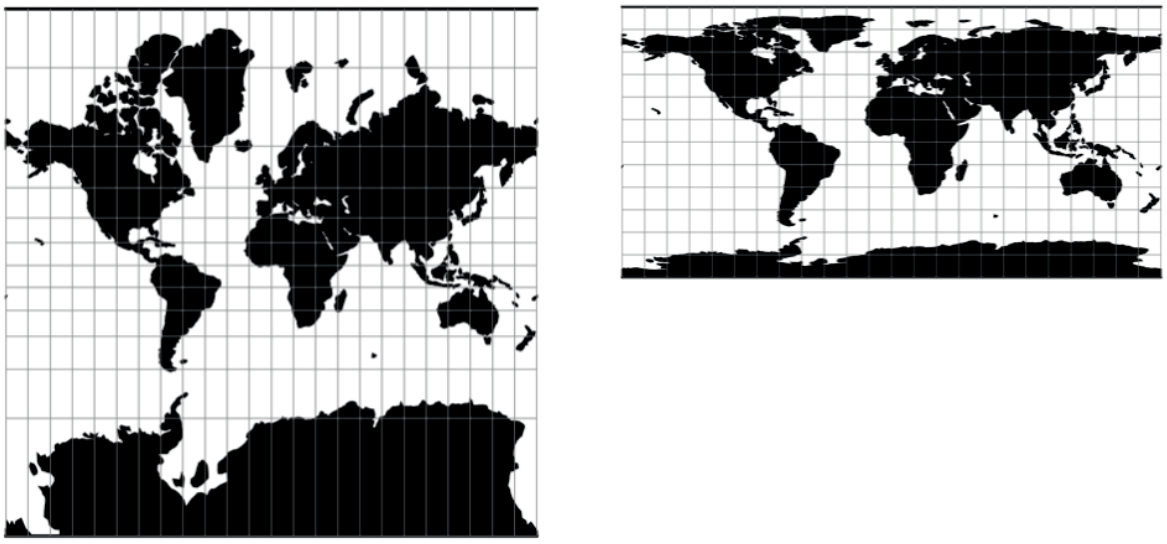

a) b)

Figure 5 *Cylindrical (a) Mercator and (b) Equidistant projections [29]*

$$x = R(\lambda - \lambda_0)\cos\phi_1,$$
$$y = R(\phi - \phi_1), \tag{11}$$

where: x is a horizontal coordinate on projected map,
y is a vertical coordinate on projected map,
R is an Earth radius in meters,
λ is a projected longitude,
λ_0 is a central map parallel,
ϕ is a projected latitude,
ϕ_1 is a standard parallel.

3.4 Accuracy evaluation

The distance between the two points must be calculated to evaluate the accuracy or error of the location determined by the techniques described in this article. On a small scale, it can be assumed that the observed surface is flat without the curvature of the Earth. The distance D between the point $P = (\lambda_1, \phi_1)$ and $Q = (\lambda_2, \phi_2)$, can be thus calculated using the simple Euclidean distance [30]:

$$D = R\sqrt{\Delta\phi^2 + (\cos\phi_m \Delta\lambda)^2}, \tag{12}$$

where: R is the radius of the Earth,
$\Delta\phi$ $|\phi_2 - \phi_1|$,
$\Delta\lambda$ $|\lambda_2 - \lambda_1|$,
ϕ_m $\frac{\phi_1 + \phi_2}{2}$.

The Euclidean distance only approximates the distance between the two geographic points if they are relatively close to each other. Since the Earth is not flat, the so-called great-circle distance must be calculated. This distance can be imagined as the length of the shortest rope laid on the Earth surface, which connects the two points, as shown in Figure 6 [30]:

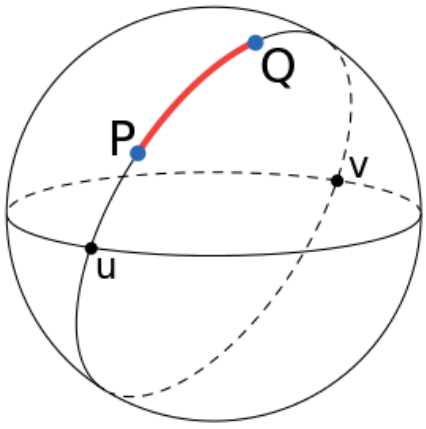

Figure 6 *Great-circle distance [30]*

$$D = R\tan^{-1}\left(\frac{\sqrt{(\cos\phi_2 \sin\Delta\lambda)^2 + +(\cos\phi_1 \sin\phi_2 - \sin\phi_1 \cos\phi_2 \cos\Delta\lambda)^2}}{\sin\phi_1 \sin\phi_2 + \cos\phi_2 \cos\phi_2 \Delta\lambda}\right) \quad (13)$$

Using this technique, it is assumed that the Earth is a perfect sphere. However, the Earth is an irregular ellipsoid. When calculating the distance between the two points, the error is never more significant than 0.5% [31]. Using Equation (13), it is possible to calculate the distance between the two points and thus verify the error rate of the geolocation methods.

3.5 Methodology of data collection and processing

Slovanet provided an end device from the manufacturer Ursalink, which periodically communicated with gateways connected to the public provider LoRaWAN network. In the private LoRaWAN network, the end device described in Section 3.1 was used during the experiments. The process of data collection was similar in both networks. To accurately record the real-time position of the end device, an external ublox GPS sensor with a precision of 15 mm placed next to the end devices was utilized during measurements, recording the position twice per second. The GPS sensor was also used to position the gateways. It is worth noting that the coordinates of the end device were processed not at the time of transmission but at the time of reception at the network server. The processing of measured data consisted of several steps:

Assignment of the recorded position by the external GPS sensor to uplink messages based on timestamps.

1. Transformation of latitude and longitude into x and y coordinates using the local cylindrical equidistant projection.
2. Determination of parameter values ($L_{PL}(d0)$ and β) for individual gateways.
3. Evaluation of the geolocation accuracy.

The data collected from both networks are visualized in Figures 7a and 7b.

During the first step the end device's location was assigned to uplink messages based on the timestamps. Since the external GPS sensor recorded its position twice per second, it often happened that the time of message reception at the network server was not precisely the same as that of the external GPS sensor. In such a case, the location was selected at the time closest to the message reception time. The difference never exceeded 500 ms.

The second step consisted of transforming the latitude and longitude coordinates into *x and y* coordinates using the local cylindrical equidistant projection. To transform the coordinates while preserving the actual scale, it was first necessary to determine ϕ_1 *and* λ_0. To verify the correctness of the so-called true scale equidistant cylindrical projection, the distance between the two most distant points in the dataset was compared using the Euclidean distance in the Cartesian two-dimensional plane and the great-circle distance. The maximum possible distance error between the two points using the Euclidean distance versus the great-circle distance was 0.000019 mm (0.0000000084 %) at a length of 228.77 m. The margin of error is small enough that it is possible to continue working with the x and y coordinates in the Cartesian plane and using the Euclidean distance.

The next step was to determine the values of the parameters ($L_{PL}(d0)$ and β) for individual gateways, laying the logarithmic curve so that it best describes the relationship between the distance and path loss. It is observed that the theoretical FSPL model, compared to the LDPL model, is highly underestimated and unsuitable for determining the location of the end device. Based on the results, it is concluded that even a tiny obstacle between the gateway and the end device results in large fluctuations in the path loss, thus significantly affecting the geolocation accuracy. After

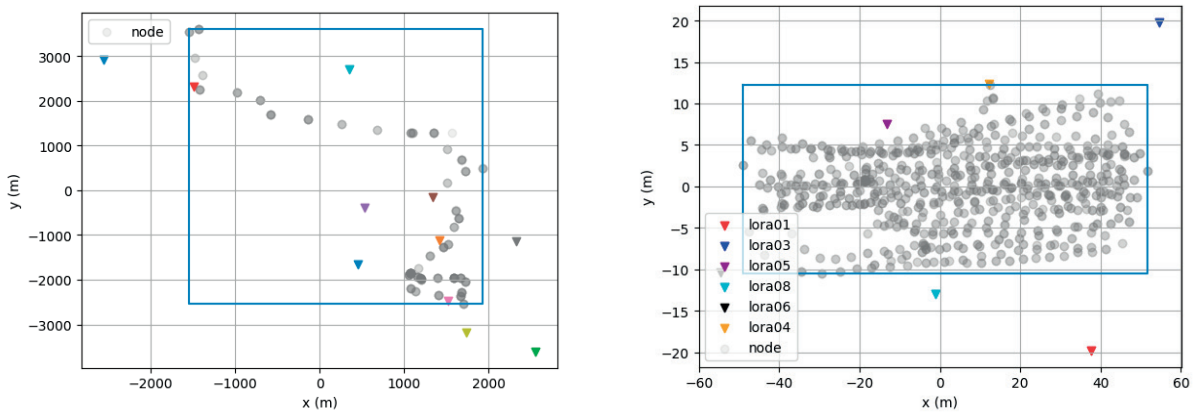

a) *b)*

Figure 7 *Visualization of measured data in (a) public provider and (b) private network using equidistant cylindrical projection*

that, the distance of the end device from the gateway using the path loss was calculated.

The penultimate step was to perform the filtering of the unsuitable uplink messages - 132 of the original 233 messages could be used for the geolocation.

In the last step the accuracy of the geolocation techniques was evaluated.

3.6 LDPL-M algorithm

To determine the location of the end device, the use of the trilateration method was proposed, i.e., to associate the distance of the end device from individual gateways based on the value of the signal loss during propagation. The reason for using this method is the insufficient time synchronization between the gateways caused by the hardware limitations. This fact does not allow to determine the position using the multilateration method.

The collected dataset has a characteristic feature - since the end device sends uplink messages regularly in a certain period, the overall geolocation accuracy can be potentially improved by incorporating the previous locations into the calculation. The condition for this approach is to know the real location of the end device at the time of sending the first message. This data can be obtained either by one of the geolocation methods or by using GPS. It is also necessary to determine how far the device will most likely move until the next message reception. The distance the device can potentially travel can be determined in two ways:

Calculate all the distances between individual uplink transmissions based on empirical measurements and then determine the largest distance that the device has traveled in 90% of cases.

Determine how fast the device usually moves and associate the distance traveled with the device's speed and the periodicity of the uplink transmission.

After defining the distance the device will most likely travel, it is proposed to use the previous location of the device as the location of an additional virtual gateway in the next transmission. The location of this virtual gateway will represent the center of a circle with a radius equal to the defined distance that the device will most likely travel. Adding the virtual gateway has the potential to improve the geolocation of the end device using the trilateration method, virtually increasing the number of gateways that have captured the message. The limitation of this method lies in the assumption that the device moves constantly, or its speed is part of movement data , i.e., known in advance, or is a part of the data payload.

In the case of a stationary device, the algorithm would worsen the measured results, since it assumes the device is in motion. Furthermore, this algorithm is not suitable for use cases where the speed of the end device changes significantly. The LDPL-M algorithm is thus proposed, its accuracy is experimentally verified on real data, and it is compared to the common trilateration methods described in previous sections. In the previous geolocation techniques, it was assumed that the end device was mobile. However, in the real-world scenarios, the situations where the end devices are stationary are often encountered. In the context of computing the end devices' location within the LoRaWAN network, this observation was leveraged to enhance the accuracy of the proposed model. To do this, a set of messages from the private LoRaWAN network was gathered, all close to each other (within a 2 m range). By doing this, a scenario

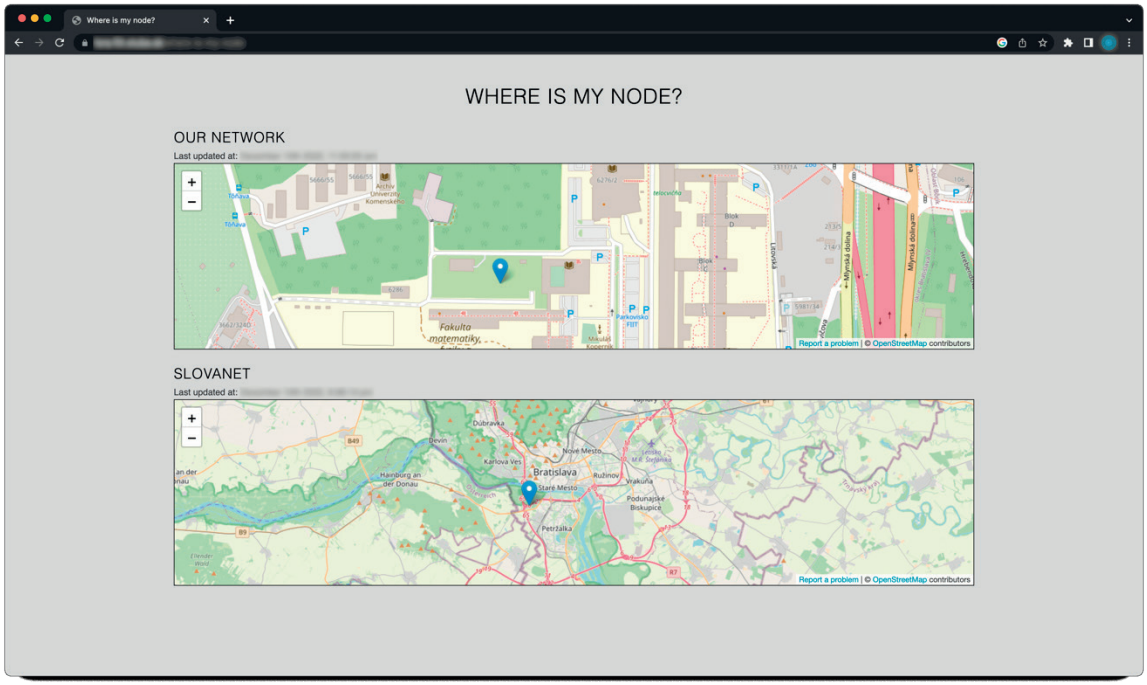

Figure 8 *User interface*

mimicking a stationary device was effectively created. In determining the stationary end device's location, the current estimation and the previous results were incorporated into the calculation. This was achieved by averaging the current estimated location with the results obtained from prior computations. To ensure stability and mitigate significant variations in the RSSI due to environmental factors, the averaging process was limited to the last N previously estimated end device's locations. This approach averages the location estimate to smooth abrupt RSSI value changes, potentially refining the geolocation accuracy for stationary end devices. It is important to note that the two different methods of averaging location exist:

1. The first way is to figure out the current location and then find the average of the locations determined before.
2. The second way is to figure out the current location and then find the average of earlier locations that had already been treated the same way (averaged). The second method provided better results.

3.7 "Where is my node ?"

The web application visualizing the end device's location is called "Where is my node ?" It is fully containerized using the Docker platform. A location update occurs every time an uplink message is received from the end device. The user interface is shown in Figure 8. It displays the timestamp of the last location update. The page overviews the geolocation from both the public provider and private LoRaWAN networks.

4 Dataset

During the measurements, a dataset from both the private and the Slovanet public provider networks was created. The ublox external GPS sensor was used to gather the precise location data, shown in Figure 9c, as a reference. The format of messages received in the public provider network slightly differs from those captured in a private network. Therefore, it was necessary to reflect this fact during the implementation of the custom parser, which combines geographical data from the external GPS sensor and uplink message based on the timestamps. The dataset is publicly available for the community at the link *https://data.ail.sk/dataset-geolora/*.

In the private network a LilyGo TTGO ESP32 end device, equipped with an SX1276 LoRa chip and built-in NEO-6M GPS module, was utilized. The end device is shown in Figure 9a. The external GPS sensor near the end device serves as a ground truth for the proposed solution verification. The data from the end devices were processed by the ChirpStack network server and forwarded in JSON format to the external application

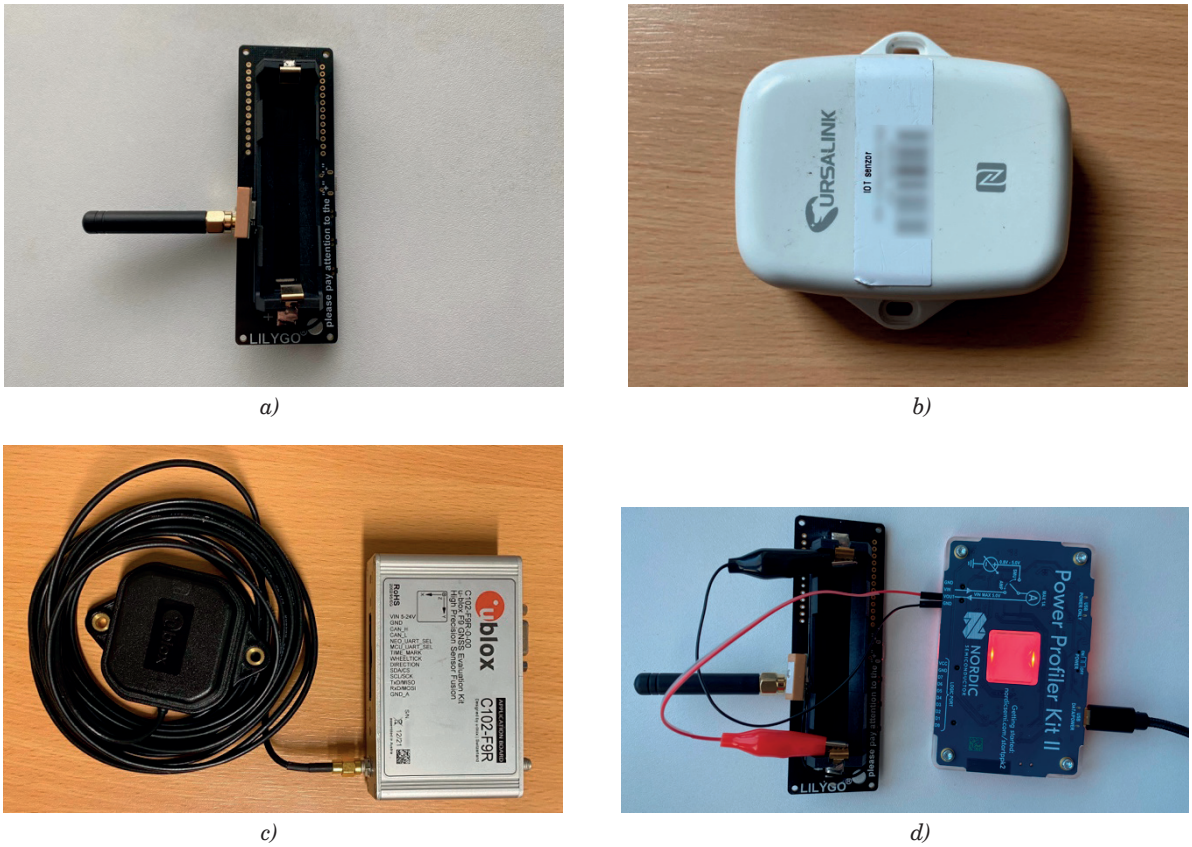

a) *b)* *c)* *d)*

Figure 9 *Hardware used during experimental setup - (a) LilyGo TTGO end device, (b) Ursalink end device, (c) ublox GPS sensor and (d) Power profiler kit II connected to the end device*

server (HTTP) via an integration functionality. The server then extracted the message reception timestamp and appended a new line to the Comma-Separated Values (CSV) file. After the extraction, the output file was combined with the GPS sensor data using a custom parser. Finally, the static information about the locations of individual gateways was appended.

In the public provider network, the end device from the manufacturer Ursalink was used, shown in Fig. 9b. Access to the data was possible during the message reception or by obtaining historical data stored in the cache. The cache stored messages for 30 days and could be downloaded via the Representational State Transfer Application Programming Interface (REST API) in JSON format at most once a day. On the other hand, the MQTT protocol allowed the subscription to the topic of interest and thus provided access during packet reception. The data was collected using the MQTT client. The uplink messages were sent by a provider with a 5-minute periodicity, and the interval could not be further modified.

The only difference worth noting, compared to the private network, was encountered when filtering messages unsuitable for geolocation. As it was not possible to access the physical topology, the packet data in the public provider network contained the location of the gateways. Not every gateway had information regarding its location available. Therefore, it was necessary to remove such gateways and then evaluate whether at least three gateways with known positions received the message to be able to apply the trilateration.

5 Results and discussion

When determining the location of the end devices, the techniques discussed in this article - FSPL, LDPL, WC, and the proposed LDPL-M - were compared to each other and the GPS data. In all cases working with the path loss, the RSSI was substituted with the ESP.

The detailed results of the error rate in the private LoRaWAN network with DLoS are shown in Figure 10 and Table 1. These results clearly show that the most accurate way to determine the location is to use the GPS sensor, which is located directly on the top of the end device but at the expense of increased power consumption. A similar average error is observed for all the discussed techniques. The difference in accuracy between the LDPL model with and without memory is more significant. The LDPL-M method improves the geolocation accuracy over the conventional LDPL model by 24.54 % in 90 % of cases. The WC results in a similar accuracy, but this method is only applicable for the geolocation within the polygon formed by the gateways. The disadvantage is that the nature of the device must be known in advance, i.e., the speed at which the device moves. This limits the possibilities of using the technique. However, the end device can also send the measured or estimated speed inside the LoRaWAN packet payload.

The detailed error results for the public provider LoRaWAN network without DLoS are shown in Figure 11 and Table 2. During this test, the device was moved around Bratislava by walking rather than staying in the reserved area defined by spread gateways. The results show that the absence of DLoS and densely built regions significantly impacted the geolocation accuracy. Depending solely on the RSSI without DLoS is unreliable. While our proposed model has improved the overall accuracy, the error rate is still high for majority of use cases.

Substituting the RSSI with the ESP proved to have a significant impact on the geolocation accuracy in the public provider network. In 90% of cases, the error rate

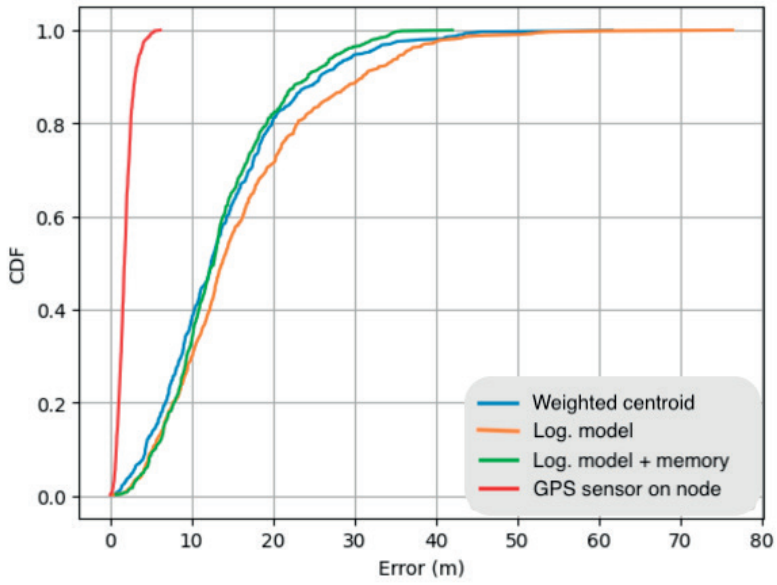

Figure 10 *Accuracy comparison in private network*

Table 1 *Error rate comparison in private network (DLoS)*

Method	*90 percentile error (m)*	*50 percentile error (m)*
GPS Sensor	3.11	1.78
LDPL-M	24.33	12.76
WC	25.80	12.43
LDPL	31.01	13.83

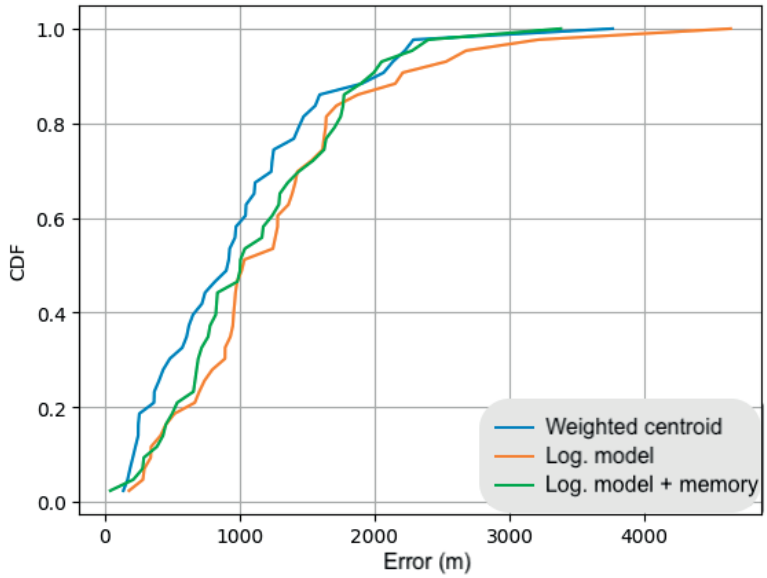

Figure 11 *Accuracy comparison in public provider network*

Table 2 *Error rate comparison in public provider network (no DLoS)*

Method	*90 percentile error (m)*	*50 percentile error (m)*
LDPL-M	1974.99	1006.42
WC	2034.64	919.51
LDPL	2197.53	1035

using the RSSI to calculate the path loss in the LDPL model was less than or equal to 2478.31 m, while using the ESP value it was 2197.53 m. Therefore, a significant improvement in determining the location by 11.35% was observed. The impact of using the ESP decreases when the device is located closer to the gateway or with DLoS, because the ESP partially considers the environmental influence on the final RSSI.

In the case of an environment with DLoS, the ESP differs minimally from the RSSI, which could be observed in the data collected in the private network. It is still advisable to use the ESP instead of the RSSI.

Regarding the modification proposed for stationary devices, Tables 3 and 4 contain the comparison of error rate between the original and modified geolocation techniques for the stationary end device. The graphs of CDF curves for individual measurements are shown in Figures 12a and 12b.

The outcomes indicate that the modified methods enhance the geolocation accuracy. The results of the previous $N = 10$ calculated locations were incorporated when averaging.

The precision of the LDPL-M algorithm increased from the initial 27.20 m to 7.56 m in 90 % of cases. Thus, it is evident that determining the location of a stationary end device is significantly more accurate than determining the position of a mobile device.

The energy consumption between scenarios with and without the active GPS module during the message transmission and reception was compared, as well. To measure the power consumption, the Power Profiler Kit II from Nordic Semiconductor [32] was utilized, connected in sequence with the end device's battery pins, shown in Figure 9d. Bundled software recorded fluctuations in current over time.

The detailed results are shown in Table 5. The measurements showed the end device's power consumption significantly increased (by an average of 48.8 %) when the GPS module was active. This finding underscores that utilization of the GPS module for the

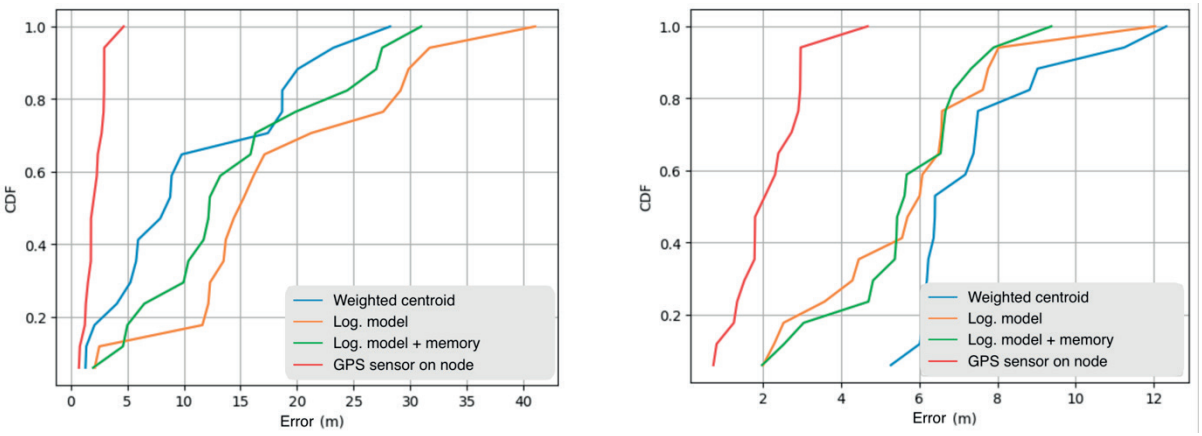

Figure 12 *Accuracy comparison of (a) original and (b) modified methods for the stationary device*

Table 3 *Error rate for stationary device using original methods in private network*

Method	*90 percentile error (m)*	*50 percentile error (m)*
LDPL-M	27.20	12.29
WC	21.31	8.79
LDPL	30.59	15.31

Table 4 *Error rate for the stationary device using original methods in private network*

Method	*90 percentile error (m)*	*50 percentile error (m)*
LDPL-M	7.56	5.62
WC	9.92	6.40
LDPL	7.87	6.01

Table 5 *GPS module power consumption measurements*

GPS module	*Average (mA)*	*Transmission (mA)*	*RX window opened (mA)*
Off	86	140	102
On	128	165	141

geolocation yields notably enhanced accuracy compared to the trilateration, but at the expense of a significantly higher power consumption.

6 Limitations and future work

Although the GPS-independent geolocation is a promising research area and the proposed solution provided reasonable results, the RSSI-based geolocation is commonly known to have its limitations.

In this section, firstly, the limitations encountered during the research are discussed. Secondly, the portability options are examined, and finally, the potential future work is described.

Limitations of the RSSI-based geolocation are tightly connected to the wireless nature of the underlying technology. The overall accuracy is affected by even more factors:

1. RSSI non-linearity or lack of DLoS. The DLoS between the gateways and the end device is important for a proper and accurate geolocation using the RSSI. Even a small obstacle results in a large path loss fluctuation, which affects the overall accuracy. Signals often reflect from the surfaces, creating multiple paths to the receiver, which also causes variations in the RSSI. Substituting the RSSI with the ESP had a significant impact on the accuracy, as it partially considers the environmental influence. This was more significant in the Slovanet public LoRaWAN network.
2. Gateway placement and density. The gateway placement and density are both crucial factors impacting the accuracy and reliability of the RSSI-based geolocation. Every end device should be placed within the range of multiple gateways, for the purposes of trilateration, at least three. The interference and multipath effect can be minimized

by placing the gateways in areas without reflective surfaces or electromagnetic noise. In addition, the overlap in coverage ensures reliability and accounts for the end device mobility. Despite the data collection process in the public provider network being very similar to the data collection in the private network, several public gateways did not provide information about their location. As access to the public infrastructure was not possible, the only option was to rely on the location data contained in the payload. Such gateways, missing the location data, had to be removed from the calculations.

3. Reliance on historical data. A standard LDPL model does not rely on historical data. On the other hand, the LDPL-M algorithm considers historical data during the calculation. The algorithm converged gradually and achieved higher accuracy with the increasing volume of collected data. The disadvantage of this approach is that if the gateway moves, the entire data collection must be repeated, and therefore, the previously collected data is unusable. Additionally, the uplink transmission periodicity can influence the accuracy.
4. Precise time synchronization. The research presented in the article was exclusively focused on the RSSI-based techniques instead of the TDoA due to the lack of precise time synchronization. Several studies show better accuracy of the TDoA over the RSSI [13, 17]. The applicability of the TDoA was limited by the hardware capabilities. The TDoA multilateration could potentially achieve higher precision; it would require the modification of the gateway hardware, as the time synchronization using the NTP proved to be insufficient for this use case.

In terms of portability, the proposed solution relies solely on the RSSI, which is contained within the LoRaWAN messages provided by the ChirpStack network server for the further operation at the application layer, and the known location of individual gateways. As long as these two prerequisites are met, the solution is independent of the underlying technology. It is still necessary to consider the above-mentioned limitations, especially the DLoS, proper placement and density of gateways, as well as the transmission periodicity.

The subject of the future work could be developing the geolocation method based on multilateration using the TDoA. This method requires modifying the gateway hardware, which must be equipped with an additional module to ensure a high degree of time synchronization between the individual gateways - in this case, the use of GPS may be appropriate, since the gateway usually has the permanent power supply, and therefore low power consumption is not as crucial as in the case of the energy-harvesting end devices.

The experiments confirmed that the geolocation using the RSSI-based trilateration is not suitable for dense urban areas without DLoS. Instead, when certain conditions are met, the proposed solution achieves better results than commonly used algorithms. The advantage is that all the calculations are performed on the server, so the solution does not negatively impact the end device's power consumption. On the other hand, the disadvantage is that the end device still has no knowledge about its location.

7 Conclusion

Geolocation of the end devices in LPWANs, while maintaining the low power consumption over a relatively large area, is a promising research area that opens up many use cases. Choosing the proper technique requires a thorough evaluation of advantages and disadvantages, especially in terms of overall efficiency.

This research was focused on the comparison of the existing techniques in both the private and public LoRaWAN networks. Next, the process of data collection and processing was described. A novel LDPL-M algorithm utilizing the end device's previous locations was proposed to enhance the geolocation accuracy, while also concerning the low power consumption. Compared to the existing techniques, the LDPL-M also considers the end device's previous locations. To assess the accuracy, the location of the end device was determined using an external GPS sensor and matched with the collected uplink messages. Part of the research was dedicated to the estimation of the end device's starting position as an input to the discussed geolocation methods. A significant environmental influence on the RSSI value was observed during the experiments. The measurements confirmed that the geolocation of end devices in the LoRaWAN network using the trilateration is possible; however, it is not suitable for densely built-up areas without DLoS. During experiments, the LDPL-M achieved better results than commonly used techniques. The impact of the GPS module on the end device's power consumption was assessed. Results revealed a notable increase with GPS enabled by an average of 48.8%, which indicates using a GPS module is significantly more accurate than the trilateration technique in LPWANs, but at the cost of higher power consumption. At the same time, a significantly lower error rate for the geolocation of a stationary end device was observed compared to a mobile device scenario. The main benefit is that the proposed solution does not require additional communication overhead, which implies it has no negative effect on the power consumption compared to the standard operation. Finally, a web application that displays the location of the end device in real time in both the private and public provider networks was implemented.

To our knowledge, there is currently no similar dataset that pairs the geographic data with uplink reports from Bratislava, Slovakia. The measurements

confirm that the environment significantly affects the RSSI. The experiments proved that the proposed LDPL-M algorithm achieves better results than the commonly used techniques under specific conditions.

Although the research was focused on the LoRa technology and the LoRaWAN protocol, the findings are not specific to the underlying technology but rather generally applicable to wireless communication technologies.

Acknowledgements

Funded by the EU NextGenerationEU through the Recovery and Resilience Plan for Slovakia under the project No. 09I05-03-V02-00012. This project has been supported by APVV-23-0137 project "Legal and technical aspects of cybersecurity situational awareness". The authors would like to thank for financial contribution from the STU Grant scheme for Support of Young Researchers. The authors would also like to express their gratitude to Slovanet, a.s. for granting access to the public provider network and borrowing the equipment necessary for the research.

Conflicts of interest

The authors declare that they have no known competing financial interests or personal relationships that could have appeared to influence the work reported in this article.

References

[1] DAWOUD, S. GNSS principles and comparison [online] [accessed 2025-04-15]. Potsdam, Germany: Potsdam University, 2012. Available from: http://www.snet.tu-berlin.de/fileadmin/fg220/courses/WS1112/snetproject/gnss-principles-and-comparison_dawoud.pdf

[2] SINHA, R., YIQIAO W., HWANG, S. A survey on LPWA technology: LoRa and NB-IoT. *ICT Express* [online]. 2017, **3**(1), p. 14-21 [accessed 2025-04-15]. eISSN 2405-9595. Available from: https://doi.org/10.1016/j.icte.2017.03.004

[3] LINK LABS A comprehensive look at low power, wide area networks [online] [accessed 2025-04-15]. 2016. Available from: https://www.link-labs.com/low-power-wide-area-networks-white-paper

[4] GARCHE, J., DYER, C. *Encyclopedia of electrochemical power sources*. Elsevier, 2009. ISBN 9780444520944.

[5] CHENEBAULT, P., VALLIN, D., THEVENIN, J., WIART, R. Impedance analysis of the lithium discharge in Li-$SOCl_2$ cells: synergetic effect of SO_2 and $LiAl(SO_3Cl)_4$. *Journal of Applied Electrochemistry* [online]. 1989, **19**(3), p. 413-420 [accessed 2025-04-15]. ISSN 0021-891X, eISSN 1572-8838. Available from: https://doi.org/10.1007/BF01015245

[6] ANJUM, M., KHAN, M. A., HASSAN, S. A., MAHMOOD, A., GIDLUND, M. Analysis of RSSI fingerprinting in LoRa networks. In: 2019 15th International Wireless Communications and Mobile Computing Conference IWCMC: proceedings [online]. 2019. ISBN 978-1-5386-7748-3, p. 1178-1183. Available from: https://doi.org/10.1109/IWCMC.2019.8766468

[7] ARAS, E., RAMACHANDRAN, G. S., LAWRENCE, P., HUGHES, D. Exploring the security vulnerabilities of LoRa. In: 2017 3rd IEEE International Conference on Cybernetics CYBCONF: proceedings [online]. 2017. ISBN 978-1-5386-2201-8, p. 1-6. Available from: https://doi.org/10.1109/CYBConf.2017.7985777

[8] LORA ALLIANCE LoRaWAN specification v1.1 [online] [accessed 2025-04-15]. 2017. Available from: https://lora-alliance.org/resource_hub/lorawan-specification-v1-1/

[9] Semtech Corporation LoRa and LoRaWAN [online] [accessed 2025-04-15]. 2024. Available from: https://www.semtech.com/uploads/technology/LoRa/lora-and-lorawan.pdf

[10] PERESINI, O., KRAJCOVIC, T. More efficient IoT communication through LoRa network with LoRa@ FIIT and STIOT protocols. In: 2017 IEEE 11th International Conference on Application of Information and Communication Technologies AICT: proceedings [online]. 2017. ISBN 978-1-5386-0502-8, p. 1-6. Available from: https://doi.org/10.1109/ICAICT.2017.8686837

[11] MONTAGNY, S. LoRa - LoRaWAN and internet of things for beginners [online] [accessed 2025-04-15]. University of Savoy Mont Blanc, 2021. Available from: https://www.univ-smb.fr/lorawan/wp-content/uploads/2022/01/Book-LoRa-LoRaWAN-and-Internet-of-Things.pdf

[12] ANJUM, M., KHAN, M. A., HASSAN, S. A., MAHMOOD, A., QURESHI, H. K., GIDLUND, M. RSSI fingerprinting-based localization using machine learning in LoRa networks. *IEEE Internet of Things Magazine* [online]. 2020, **3**(4), p. 53-59 [accessed 2025-04-15]. ISSN 2576-3180, eISSN 2576-3199. Available from: https://doi.org/10.1109/IOTM.0001.2000019

[13] FARGAS, B., PETERSEN, M. GPS-free geolocation using LoRa in low-power WANs. In: 2017 Global Internet of Things Summit GIoTS: proceedings [online]. 2017. ISBN 978-1-5090-5874-7, p. 1-6. Available from: https://doi.org/10.1109/GIOTS.2017.8016251

[14] PODEVIJN, N., PLETS, D., AERNOUTS, M., BERKVENS, R., MARTENS, L., WEYN, M., JOSEPH, W. Experimental TDoA localisation in real public LoRa networks. In: 10th International Conference on Indoor Positioning and Indoor Navigation IPIN 2019: proceedings [online] [accessed 2025-04-15]. 2019. p. 211-218. Available from: https://ceur-ws.org/Vol-2498/short28.pdf

[15] ZUCCONI, A. Positioning and trilateration [online] [accessed 2025-04-15]. 2017. Available from: https://www.alanzucconi.com/2017/03/13/positioning-and-trilateration/

[16] OGUEJIOFOR, O., ANIEDU, A. N., EJIOFOR, H. C., OKOLIBE, A. U. Trilateration based localization algorithm for wireless sensor network. *International Journal of Innovative Science and Modern Engineering (IJISME)* [online]. 2013, **1**(10). p. 21-27 [accessed 2025-04-15]. ISSN 2319-6386. Available from: https://www.ijisme.org/wp-content/uploads/papers/v1i10/J04470911013.pdf

[17] LESTABLE, T., LALAM, M., GRAU, M. Location-enabled LoRa IoT network: Geo-LoRa-ting your assets [online] [accessed 2025-04-15]. 2015. Available from: https://www.slideshare.net/slideshow/io-t-sagemcom-m2minnovationworldgeotrackv08/52922413

[18] RUSLI, M., ALI, M., JAMIL, N., DIN, M. M. An improved indoor positioning algorithm based on RSSI-trilateration technique for internet of things (IOT). In: 2016 International Conference on Computer and Communication Engineering ICCCE: proceedings [online]. 2016. ISBN 978-1-5090-2428-5, p. 72-77. Available from: https://doi.org/10.1109/ICCCE.2016.28

[19] YANG, Z., LIU, Y. Quality of trilateration: confidence based iterative localization. In: 2008 The 28th International Conference on Distributed Computing Systems: proceedings [online]. 2008. ISSN 1063-6927, p. 446-453. Available from: https://doi.org/10.1109/ICDCS.2008.59

[20] Semtech Corporation AN1200.22 LoRa modulation basics [online] [accessed 2025-04-15]. 2015. Available from: https://www.frugalprototype.com/wp-content/uploads/2016/08/an1200.22.pdf

[21] BISSET, D. Analysing TDoA localisation in LoRa Networks. Master's thesis [online] [accessed 2025-04-15]. Delft: TU Delft, Faculty of Electrical Engineering, Mathematics and Computer Science, 2018. Available from: https://resolver.tudelft.nl/uuid:bea423b1-6f04-4708-8ed4-e8663dd51cde

[22] GARG, V. *Wireless communications and networking*. San Francisco, CA: Morgan Kaufmann Publishers, Inc. 2010. ISBN 9780080549071.

[23] JORKE, P., BOCKER, S., LIEDMANN, F., WIETFELD, CH. Urban channel models for smart city IoT-networks based on empirical measurements of LoRa-links at 433 and 868 MHz. In: 2017 IEEE 28th Annual International Symposium on Personal, Indoor, and Mobile Radio Communications PIMRC: proceedings [online]. 2017. ISBN 978-1-5386-3532-2, p. 1-6. Available from: https://doi.org/10.1109/PIMRC.2017.8292708

[24] VALACH, A., MACKO, D. Exploration of the LoRa technology utilization possibilities in healthcare IoT devices. In: 2018 16th International Conference on Emerging eLearning Technologies and Applications ICETA: proceedings. 2018. ISBN 978-1-5386-7915-9, p. 623-628.

[25] RAHMADHANI, A. Performance evaluation of LoRaWAN: from small-scale to large-scale network. Master's thesis [online] [accessed 2025-04-15]. Delft: TU Delft, Faculty of Electrical Engineering, Mathematics and Computer Science. 2017. Available from: https://resolver.tudelft.nl/uuid:b8acf9d3-9629-4439-9148-9e66aecbec1c

[26] PARENTE, L. LMIC-node - GitHub [online] [accessed 2025-04-15]. 2021. Available from: https://github.com/lnlp/LMIC-node

[27] BROCAAR, O. ChirpStack, open-source LoRaWAN Network Server [online] [accessed 2025-04-15]. 2016. Available from: https://www.chirpstack.io/

[28] SNYDER, J. Map projections: a working manual. Professional Paper 1395 [online] [accessed 2025-04-15]. 1987. Available from: https://doi.org/10.3133/pp1395

[29] Proj Contributors Proj coordinate transformation software library - Open Source Geospatial Foundation [online] [accessed 2025-04-15]. 2025. Available from: https://doi.org/10.5281/zenodo.5884394

[30] ZUCCONI, A. Understanding geographical coordinates [online] [accessed 2025-04-15]. 2017. Available from: https://www.alanzucconi.com/2017/03/13/understanding-geographical-coordinates/

[31] Great Britain. Ministry of Defence (NAVY) *Admiralty manual of navigation*. The Stationery Office, 1987, 1(45). ISBN 9780117714687.

[32] Nordic Semiconductor Power Profiler Kit II [online] [accessed 2025-04-15]. 2024. Available from: https://www.nordicsemi.com/Products/Development-hardware/Power-Profiler-Kit-2